The 2010 IEEE/RSJ International Conference on
Intelligent Robots and Systems
October 18-22, 2010, Taipei, Taiwan

Stability and Adaptability of Passive Creeping of a Snake-like Robot

Zhifeng Wang, Shugen Ma, Bin Li, and Yuechao Wang

Abstract— **The control of a snake-like robot is a challenging problem because of the complex dynamics and the unknown environment. We have proposed an energy-based method, called *passive creeping*, to control the serpentine locomotion. This paper lays emphasis on the stability and the adaptability of the method. First, the local orbital stability of the movement is explicated based on the maximal Lyapunov exponent and the recurrence plot. Second, the adaptability to the environment is analyzed, and an optimal adaptive law based on the energy proportion is put into use to perfect the method. The particular advantages of the passive creeping include the comprehensive concept, the explicit control, and the inherent adaptability.**

I. INTRODUCTION

A snake can perform various locomotion gaits, e.g. serpentine locomotion, according to different environments ([1]), so the snake has great environment adaptability. A snake-like robot has this merit potentially by imitating the snake. However, these characteristics, such as the redundant degrees of freedom (DOFs), and the interaction between the robot and the environment, make the dynamics of the robot very complicated. Thus, it is difficult to construct an effective control method for the snake-like robot.

Many researchers focus their interests on the serpentine locomotion to increase the environment adaptability of the snake-like robot. The existing control modes of the locomotion can be mainly divided into three categories [2]. First, the curve based method controls the joint angles fitting a reference curve to shape the robot [1], [3]. The method produces diverse gaits easily, but the parameter changing and gait transforming are clumsy and discontinuous. Second, the model based method includes the rigid-body-model based method [4] and the continuum-model based method [5]. The limitation is that the dynamic model is too complicated, and some predigested conditions are disabled in a real environment. Third, the CPG based method uses nonlinear differential equations to generate rhythmical traveling waves [2], [6], [7]. The sensory information can be integrated into the method. However, modulating the parameters for different gaits is difficult, because of the intractability of the nonlinear equations.

The mentioned methods neglect the energy effect in the serpentine locomotion. We have presented passive creeping integrating the energy-based control with the basic gait to control the snake-like robot in [8]. Comparing to the previous work, we analyze the orbital stability and the environment adaptability of the passive creeping, and propose an optimal adaptive law to perfect the method in this paper. The work can be considered as a step toward insightfully understanding and effectively controlling the serpentine locomotion. According to the analysis in the paper, we can summarize the advantages of the passive creeping as follows: 1) The concept of the method including the environment effect, dynamics effect and generalized gait is comprehensive; 2) The control strategy is explicit, because that regulating the input torque, evaluating the locomotion and constructing the adaptive law all focus on the kinetic energy; 3) The robot adapts to the environments according to the energy state inherently, without measuring the environments or computing the dynamics.

II. CONCEPT OF PASSIVE CREEPING

The snake-like robot is an articulated mechanical system as shown in Fig. 1. The length, mass, and inertia tensor of the ith module ($i = 3,\ldots,n$. The 1st and 2nd module are not referred to in the paper. See [9] for details) are l_i, m_i, and I_i^b, respectively. The configuration in coordinates can be written as $x = \left[x^1, x^2, x^3, x^4, \ldots, x^n\right]^{\mathrm{T}}$, where $\left[x^1, x^2, x^3\right]^{\mathrm{T}}$ is the position and orientation in the inertial coordinates, and $\left[x^4, \ldots, x^n\right]^{\mathrm{T}}$ represents the relative joint angles.

The concept of the passive creeping is recalled in the section, and the details can be found in [8]. The kernel of the method is the energy point of view. The kinetic energy of the snake-like robot relates with the following aspects of the serpentine locomotion.

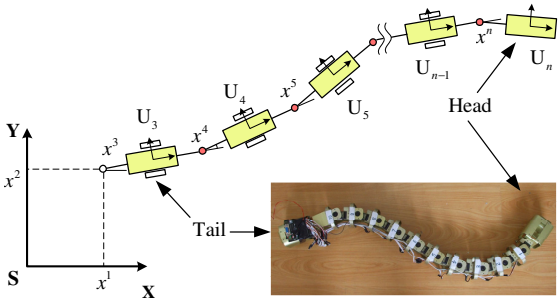

Fig. 1. Mechanism of a snake-like robot with passive wheels, but the head module is not installed the wheel.

This work is supported by the Knowledge Innovation Program of Chinese Academy of Sciences 07A1200101 and the National High Technology Research and Development Program of China (863 Program) 2006AA04Z254

Z. Wang is with State Key Laboratory of Robotics, Shenyang Institute of Automation, Chinese Academy of Sciences, Shenyang 110016, China. He is also with Graduate University of Chinese Academy of Sciences, Beijing 100039, China zfwang@sia.cn

S. Ma is with the Department of Robotics, Ritsumeikan University, Shiga-ken 525-8577, Japan. He is also with State Key Laboratory of Robotics, Shenyang Institute of Automation, Chinese Academy of Sciences, Shenyang 110016, China shugen@se.ritsumei.ac.jp

B. Li and Y. Wang are with State Key Laboratory of Robotics, Shenyang Institute of Automation, Chinese Academy of Sciences, Shenyang 110016, China libin@sia.cn; ycwang@sia.cn

First, the energy dissipation relates to the friction interaction. We describe the interaction effect between the robot and the environment by using Coulomb friction as

$$f_i = \left[-\mu_c^t m_i g \cdot \mathrm{sgn}(v_{s,i}^t), -\mu_c^n m_i g \cdot \mathrm{sgn}(v_{s,i}^n)\right] \tag{1}$$

for $i = 3, \ldots, n-1$, where 1) $v_{s,i}^t$ and $v_{s,i}^n$ are the tangent and the normal velocity along the robot's body respectively; 2) g is the gravitational acceleration. 3) μ_c^t and μ_c^n are the friction coefficients in the tangent and the normal direction respectively. Essentially, μ_c^t is the dimensionless coefficient of rolling friction (CRF) of the passive wheel, and μ_c^n is the coefficient of kinetic friction, so μ_c^n is one or two orders of magnitude bigger than μ_c^t. The dissipative power of the energy led by the interaction effect can be written as

$$P_d = \sum_{i=3}^{n-1} \left(\mu_c^n m_i g \left|v_{s,i}^n\right| + \mu_c^t m_i g \left|v_{s,i}^t\right|\right). \tag{2}$$

Second, the energy transformation relates to the dynamics of the serpentine locomotion. When the snake-like robot winds the body continuously in order to push itself onwards, the rotational kinetic energy E_R transforms to the translational kinetic energy E_T. These two kinds of energy can be defined as

$$E_R = \frac{1}{2}\sum_{i=3}^{n}\left(\omega_{s,i}^b\right)^T I_i^b \omega_{s,i}^b,\ E_T = \frac{1}{2}\sum_{i=3}^{n} m_i \left(v_{s,i}^b\right)^T v_{s,i}^b. \tag{3}$$

where $\omega_{s,i}^b$ and $v_{s,i}^b$ are the angular and the linear velocity component of the body velocity of the ith module respectively. E_T is directly correlated with the forward velocity of the robot along the trajectory. The proportion of the translational kinetic energy to the whole kinetic energy η_2 is a special quantity describing the efficiency of the serpentine locomotion in a stable state, and can be written as

$$\eta_2 = \frac{E_T}{E_R + E_T}. \tag{4}$$

Third, the serpentine locomotion relates to the energy balance among the numerous joints, because the locomotion is the resulting effect of the movements in many joints. Biologically, the head-to-tail undulatory wave along the body propels a snake onwards. The phase order of the joint angles can be found from the snake motion clearly. According to the priori knowledge, dynamic shift is proposed as

$$\tau_{n-i} = A_{n-i}\left(x^{n-i+1}(t) - x^{n-i}(t)\right) \tag{5}$$

for $i = 1, \ldots, n-4$, where A_{n-i} is a proportional coefficient. The latter joint is impelled to follow the former. The dynamic shift considered as a generalized gait expects to realize the synchronization of the joint movements. In [5], Date et al. deduced the joint torque being similar to (5) mathematically.

The concept of the passive creeping is depicted in Fig. 2. The dynamic shift produces the serpentine locomotion tendency; the environment affects the movement through the energy dissipation; and the robot dynamics influence the motion through the energy transformation.

Accordingly, we propose a control method of the snake-like robot integrating the dynamic shift with the energy-based

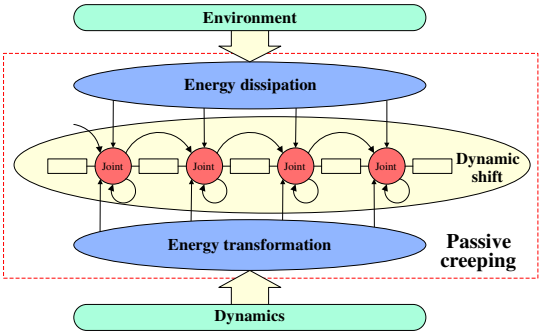

Fig. 2. Concept of the passive creeping combining the energy point of view and the basic property of the serpentine locomotion.

feedback as shown in Fig. 3. The mathematic equations of the passive creeping control are as follows.

□ Control torque of head joint:

$$\begin{aligned}\tau_n = & aI_n \left| K_n \left(\int_0^t (E_{\mathrm{ref}} - E)dt \right) + E_{\mathrm{ref}} - E \right| \\ & \cdot \left(\ddot{x}_d^n + k_d \left(\dot{x}_d^n - \dot{x}^n \right) + k_p \left(x_d^n - x^n \right) + \varphi_t \right)\end{aligned} \tag{6}$$

□ Control torque of body joint:

$$\tau_{n-i} = K_{n-i} \left(\int_0^t (E_{\mathrm{ref}} - E)dt \right) \left(x^{n-i+1} - x^{n-i} \right) \tag{7}$$

for $i = 1, \ldots, n-4$, where 1) a, k_d, and k_p are three coefficients; 2) I_n is the moment of inertia of the head module around the head joint axis; 3) $K = \left[K_n, K_{n-1}, \ldots, K_4\right]^T$ is a vector of the integrating amplification factors; 4) x_d^n is a reference angle of the head joint; 5) φ_t is a turning parameter; 6) E_{ref} and E are the reference and the real mechanical energy respectively. The reference energy E_{ref} is used to adapt to the various environments, but it is considered as an ordinary control parameter before an adaptive law is proposed.

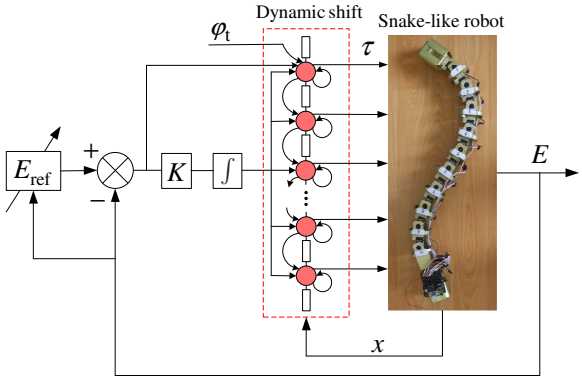

Fig. 3. Elementary control of the passive creeping. The generation of the basic movement tendency is distributed in the bottom layer; the adaption to the environment is concentrative in the middle layer; and the head joint is affected by an external excitation to lead the locomotion in the top layer.

The head joint torque τ_n implements the top-level control, such as turning, and is based on the computed torque control. $\left|K_n \left(\int_0^t (E_{\mathrm{ref}} - E)dt\right) + E_{\mathrm{ref}} - E\right|$ which is PI control has two functions as: 1) compensating the steady energy error because of the integral part, and 2) quickening the startup

TABLE I

BASIC PARAMETER OF SIMULATION STUDY

Parameter name	Symbol	Value
Number of real units	$n' = n-2$	10
Length of the ith unit	l_i	0.08 m
Mass of the ith unit	m_i	0.50 kg
Inertia of the ith unit	I_i^b	0.00027 kg·m^2
Time step of simulation	T	0.01 s
Reference angle	x_{d}^n	$0.5\sin(2t+\pi/2)$ rad
	a	10.0
	k_{d}	1.0
	k_{p}	1.0
Other factors	$\begin{bmatrix} K_n \\ K_{n-1} \\ \vdots \\ K_4 \end{bmatrix}$	$\begin{bmatrix} 0.10 \\ 0.04 \\ \vdots \\ 0.04 \end{bmatrix}$

Each real unit of the snake-like robot is of the same length, mass, and inertia respectively. In addition, the physical parameters are based on the snake-like robot in SIA, and the control coefficients are empirical.

due to the proportional term. Correspondingly, the body joint torques τ_{n-i}'s realize the serpentine locomotion. The energy error integral $\int_0^t (E_{\mathrm{ref}} - E)dt$ has the following two functions: 1) adjusting the amplitude of the body joint based on the energy control, and 2) adapting the body wriggling amplitude to the uncertain environment. To distinguish the different tasks of the head and the body module, the passive wheel is not installed on the head module as shown in Fig. 1.

The passive creeping is studied sequentially in a simulation environment based on Open Dynamics Engine (ODE). The basic fixed parameters of the simulations are presented in Table I. The variable parameters are the environment parameters (i.e., μ_{c}^n and μ_{c}^t) and the control parameters (i.e., E_{ref} and φ_{t}). The effect of the turning parameter on the serpentine locomotion is explicit. If $\varphi_{\mathrm{t}} = 0$, the robot moves straight. Otherwise, the robot turns right or left. For convenience, a triple $(E_{\mathrm{ref}}, \mu_{\mathrm{c}}^n, \mu_{\mathrm{c}}^t)$ is used to denote the variable parameters when the turning parameter φ_{t} is zero.

III. STABILITY OF PASSIVE CREEPING

By comparing the configurations, torques and angles in the initial stage with those in the final state in Fig. 4, the movement of the passive creeping is a dynamic process from an unordered state to an ordered state. The energy can reach the reference value with fluctuation, but cannot converge at it as shown in Fig. 5. This is because that the head swing which is a persistent exciting effect leads the fluctuation, and the control law cannot forecast the complex relationship between the swing and the fluctuation. The slight energy fluctuation is intricate but endurable in the serpentine locomotion.

The stability in the sense of Lyapunov is most acceptable. However, the following difficulties, e.g., energy fluctuation, nonlinear high-dimensional dynamics, and nonexistence of a fixed-frequency orbit, make it hardly to use the analytical method to prove the stability. We use the maximal Lyapunov exponent λ to describe the stability of the passive creeping.

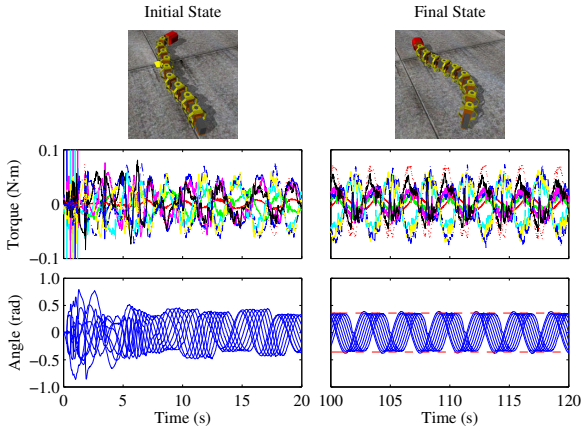

Fig. 4. Initial creeping state and final creeping state with the variable parameters (0.5, 0.50, 0.010). (See the attached video for more details.)

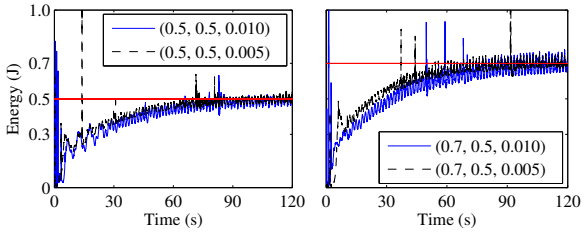

Fig. 5. Kinetic energy of the snake-like robot under the passive creeping.

The exponent is a quantity that characterizes the exponential rate of divergence or convergence of infinitesimally close trajectories in a phase space [10]. Because the joint movements which represent the locomotion mode are interested, the position and orientation of the robot in the inertial coordinates are not included in the phase space. Therefore, the movement state in the phase space can be written as $z = [x^4, \ldots, x^n, \dot{x}^4, \ldots, \dot{x}^n]$. Quantitatively, λ is determined by

$$\delta(t) \simeq \delta(0) e^{\lambda t} \tag{8}$$

where $\delta(t) = \|z_1(t) - z_2(t)\|_\infty$ is the distance some time t ahead between the two trajectories emerging from two close initial points $z_1(0)$ and $z_2(0)$. According to (8), we estimate λ as shown in Fig. 6. At the initial stage (A), the system is divergent, because the energy is injected by the motors. After startup (B), the energy is also injected, while the environment friction leads the dissipation. Wholly, the energy of the system is increased (Fig. 5). The serpentine locomotion is gradually established and rhythmized under the persistent excitation of the passive creeping at this stage, so $\lambda < 0$ and the phase volume decreases. At the final stage (C), the injected and the dissipated energy are in a dynamic balance, so $\lambda \approx 0$ and the phase volume is invariable. A limit cycle is generated in the phase space finally. Therefore, the passive creeping with certain parameters is locally orbit-stable.

The above method is suitable for the qualitative analysis not the quantitative, because of nonexistence of a fixed frequency orbit and the non-visualization of the high dimensional space. A recurrence plot (RP, [11]) can investigate the high-dimensional phase trajectory through bringing out the

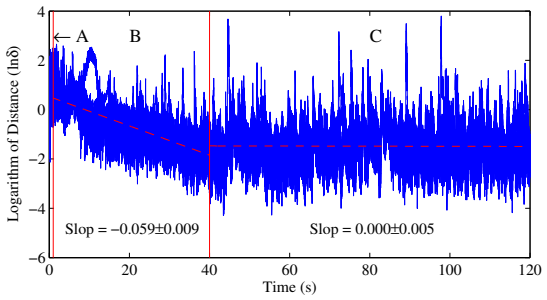

Fig. 6. Estimation of the maximal Lyapunov exponent λ of the passive creeping with the variable parameters (0.5, 0.50, 0.010). In the logarithmic presentation of the distance $\delta(t)$ over time, the slope of the fitted regression line (dashed) corresponds to λ. From nine distance sequences, the estimations for λ's in the time intervals (B) and (C) are at -0.059 ± 0.009 (mean±SD) and 0.000 ± 0.005, respectively.

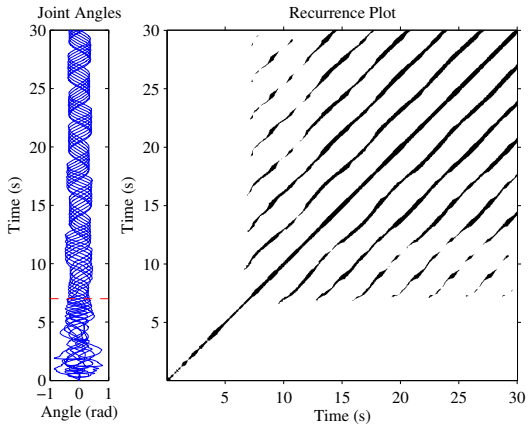

Fig. 7. Recurrence plot (right) of the joint angles (left) of the passive creeping with the variable parameters (0.5, 0.50, 0.010). In the RP, a black dot is plotted at the coordinates (i, j), if $R(i, j) = 1$ (i.e., $y(i)$ is in the ε-neighborhood of $y(j)$); and a white dot is plotted, if $R(i, j) = 0$.

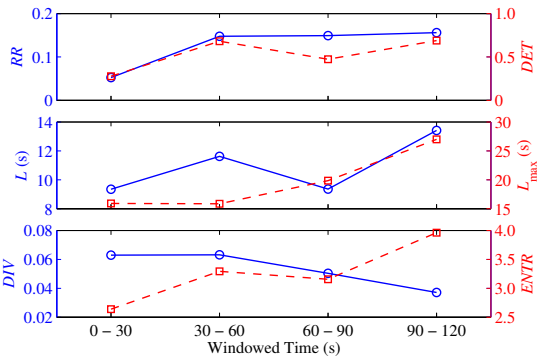

Fig. 8. Windowed recurrence quantification analysis of the passive creeping with the variable parameters (0.5, 0.50, 0.010) in the different stages. "Real line plus circle" relates to the left items, and "dashed line plus square" relates to the right. *RR*, recurrence rate, means the probability of a state recurring to its ε-neighborhood; *DET*, determinism, is a measure for the determinism of the system; *L*, averaged diagonal line length, means the average prediction time related to the divergence of the trajectory; L_{max}, the longest diagonal line, means the exponential divergence of the trajectory; *DIV*, divergence, is the inverse of the longest diagonal line relating to the exponential divergence; *ENTR*, Shannon entropy, means the complexity of the RP in respect of the diagonal lines.

recurrence of states in a time series. The RP is shaded within a two-dimensional square matrix with black and white dots to visualize the recurrence. The black dot at (i, j) marks the recurrence of the state between the time i and the different time j. The mathematical expression of the RP is as

$$R(i,j) = \Theta\left(\varepsilon - \|y(i) - y(j)\|_\infty\right) \tag{9}$$

where $y(i) = \left[x^4(i), x^5(i), \ldots, x^n(i)\right]^{\mathrm{T}}$ with the embedding dimension $n-3$, $\Theta(\cdot)$ is the Heaviside step function, and ε is a threshold distance with $\varepsilon = 0.2$ (rad). The RP of the time series of the passive creeping is plotted in Fig. 7, and the black diagonal lines (meaning the periodic recurrence) distinctly indicate that the snake-like robot implements the stable coordinate movement after the 7th second. In essence, the recurrence of the states in the phase space suggests the Poisson stability. Furthermore, recurrence quantification analysis quantifies the small scale structures in the RP beyond the visual impression. According to the quantitative analyses of the passive creeping in the different stages as shown in Fig. 8, we can conclude that: 1) The determinism of the movement (*DET*, *L*, and L_{max}) is increased, and the divergence of the trajectory (*DIV*, or the reciprocal of *L* and L_{max}) is decreased. That is, the passive creeping becomes insensitive to the initial conditions, and is robust-stable to some extent. 2) The recurrence and correlation among the joint movements (*RR* and *ENTR*) is increased in creeping. This means the synchronization is established gradually, and the energy assignment becomes balanced. Note that the stability of the passive creeping concluded from the above analyses is local but not global. These numerical methods are compromises before an analytic approach is useable.

IV. ADAPTABILITY OF PASSIVE CREEPING

On the foundation of stability, we analyze the adaptability of the passive creeping to the environments with the variable parameters varying over a broad range. The variations of the average joint angle amplitude, the average energy error integral, and the average energy proportion in the stable stage are plotted in Fig. 9. The following conclusions can be obtained as: 1) The bigger reference energy E_{ref} leads to the bigger angle amplitude and error integral, but the smaller energy proportion wholly. 2) The smaller tangential Coulomb friction coefficient μ_{c}^t results in the smaller angle amplitude and error integral, but the bigger energy proportion. 3) When the normal Coulomb friction coefficient μ_{c}^n is big enough to sustain the serpentine locomotion, the angle amplitude and the energy proportion are almost invariable with the different E_{ref}'s, and μ_{c}^n can hardly influence the three values here. 4) When μ_{c}^n is too small to sustain the locomotion, the snake-like robot skids sideways on the slippery ground. Here, the angle amplitude increases, the energy proportion decreases, and the error integral undulates acutely. 5) The bigger E_{ref} is set, the more easily the robot skids, and the bigger μ_{c}^n is needed to avoid skidding. In short, the reference energy describes the intensity of the serpentine locomotion; the tangential friction decides the performance of the movement; and the normal friction sustains the movement.

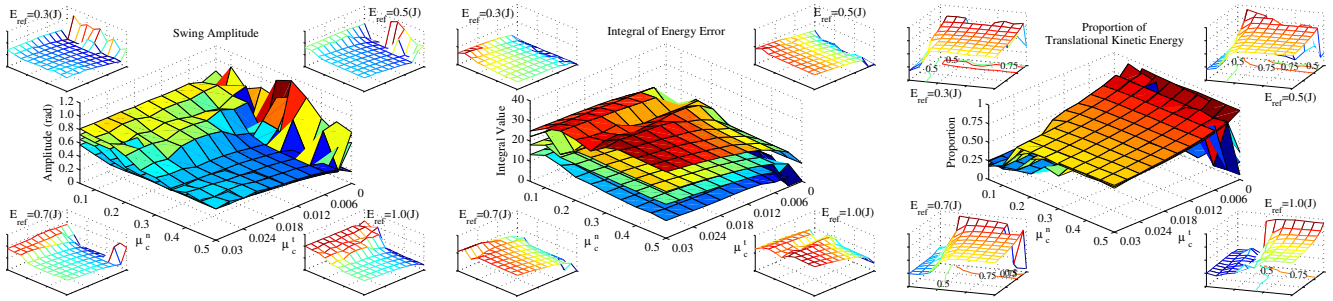

(a) Average amplitude of joint angles (b) Average integral of energy error (c) Average proportion of kinetic energy

Fig. 9. The variations of the average amplitude of joint angles (a), the average integral of energy error (b), and the average proportion of kinetic energy (c) with the variations of the control and environment parameters $(E_{\text{ref}}, \mu_{\text{c}}^n, \mu_{\text{c}}^t)$. E_{ref} is set at 0.3(J), 0.5(J), 0.7(J), or 1.0(J), experientially. μ_{c}^n and μ_{c}^t vary in the range of $[0.05, 0.50]$ and the range of $[0, 0.030]$, respectively. The ranges of the friction coefficients are based on the variation of the coefficient of kinetic friction between the wheel (rubber) and the floor, and the variation of the dimensionless coefficient of rolling friction of the passive wheel (bearing), respectively. The value of each point is the average in the stable state of the passive creeping during the time ranged $[100, 120]$ second. Each centric subfigure is packed by the four ones in the corners. In (c), the contours of the energy proportion at 0.50 and 0.75 are plotted in the corner subfigures.

Before skidding, the different environments with the different friction coefficients are all same to the snake-like robot, because the environments sustain the robot to creep alike. Even the environment force can not be calculated from the dynamic equations, because the environment interaction is overconstrained (i.e., there are many contact points on the robot interacting with the environment at the same time). On the other hand, when the movement of the robot is too violent and the environments can not sustain the movement, the different environments behave disparately because of the different upper bounds of the push force affording by the environments (See (1)). The movement capability decreases acutely, once the robot begins to skid as shown in Fig. 10.

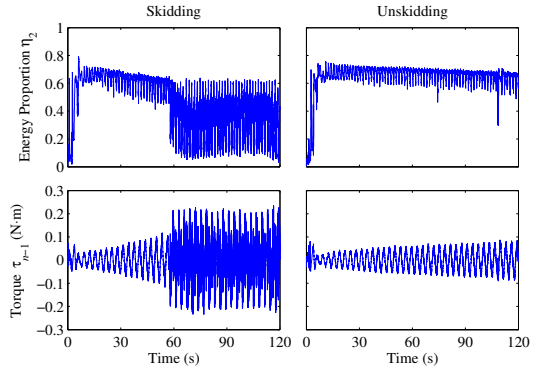

Fig. 10. Comparison of the energy proportion and the joint torque between the skidding movement and the unskidding. The left column starts to be in skidding at about the 55th second with the variable parameters $(1.3, 0.30, 0.012)$. The right column is always in unskidding with the variable parameters $(1.0, 0.30, 0.012)$.

Observing Fig. 10, when the snake-like robot skids, the average energy proportion decreases sharply and the torque amplitude increases greatly. Although the torque amplitude in the skidding sample is more than twice as big as that in the unskidding, the translational kinetic energy of the skidding one (0.4869 (J)) is much less than that of the unskidding (0.6464 (J)). Therefore, the skidding is a danger to the serpentine locomotion. How can the snake-like robot avoid skidding and optimally adapt to the different environments? Apparently, the robot can not try to measure the environment directly, because the real environment is too complex. Additionally, the robot can not compute the environment force in real time, because of overconstraint. The average energy proportion $\bar{\eta}_2$ is selected to use in the optimal adaptation, but not the torque amplitude (which was used to detect the friction coefficient in [7]). The reasons are listed as follows: 1) The average energy proportion is dimensionless with a normalized variation range $[0, 1]$, but the torque amplitude is of the range $[0, \infty)$. The change of the former can be estimated more easily. 2) The average energy proportion, relating to the energy transformation in the stable state, can be directly used in the energy optimization.

Accordingly, the concepts "skid" and "efficient" of the serpentine locomotion of the snake-like robot are quantified by the average energy proportion $\bar{\eta}_2$ as

Rule I: If $\bar{\eta}_2 < 0.50$, then the snake-like robot skids.

Rule II: If $\bar{\eta}_2 > 0.75$, then the creeping is efficient.

Rule II is mostly based on Rule I and observation (Fig. 9(c)). Now, we explain Rule I qualitatively as follows:

From the basic assumption of the snake-like robot (i.e., friction anisotropy), we obtain that $\mu_{\text{c}}^n \gg \mu_{\text{c}}^t$. When in the unskidding movement, $v_{s,i}^n = 0$; and when in the skidding movement, $v_{s,i}^n$ and $v_{s,i}^t$ are supposed in the same order of magnitude, so $\mu_{\text{c}}^n m_i g |v_{s,i}^n| \gg \mu_{\text{c}}^t m_i g |v_{s,i}^t|$. Therefore, when the robot skids, the dissipative power P_{d} greatly increases (See (2)). The control of the passive creeping attempts to hold the kinetic energy E invariable. Consequently, the torque τ must increase, and the rotational kinetic energy E_{R} increases. On the other hand, the upper bound of the friction is invariable in the same environment whether the robot skids or not (from (1)), so the forward push force acting on the robot is invariable almost. Consequently, the translational energy E_{T} can not increase when skidding. Furthermore, because E_{R} increases and E holds invariable, E_{T} can only decrease. According to (4), the energy proportion η_2 will greatly decrease when the snake-like robot skids. In addition, the range of η_2 being $[0, 1]$ and the variation of $\bar{\eta}_2$ in Fig. 9(c) make us to experientially set the critical value at 0.5.

According to Rule I, the adaptive method is designed to perfect the passive creeping as shown in Fig. 3. Only the reference energy E_{ref} can be use to construct an optimal adaptive law for the environments as follows,

$$\begin{aligned} \max \quad & E_{\text{ref}} \\ \text{s.t.} \quad & \bar{\eta}_2 \geq 0.5 \\ & (E_{\text{ref}} + \Delta E_{\text{ref}})\,(\bar{\eta}_2 + \Delta\bar{\eta}_2) > E_{\text{ref}}\bar{\eta}_2 \end{aligned} \tag{10}$$

where ΔE_{ref} is the turning value of E_{ref} such that the robot tentatively adapts to the unknown environment, and $\Delta\bar{\eta}_2$ is the change of $\bar{\eta}_2$ with the turning of E_{ref}. The first constraint is used to avoid skidding according to Rule I, and the second insures the average translational kinetic energy $\bar{E}_{\text{T}}$ increased. In fact, after the transient process, $\bar{E}_{\text{T}} \approx E_{\text{ref}}\bar{\eta}_2$. The adaptive law (10) searches E_{ref} so as to $\bar{E}_{\text{T}}$ maximal apparently. In essence, the law searches the most intensive movement in the range of the movements which the environment can sustain. Thus, the adaptive law is disabled when the environment is too slippery to sustain any serpentine locomotion.

We explain the optimal adaptive law by using an example as shown in Fig. 11. The robot implements the passive creeping in an unknown environment. Initially, the robot is skidding in Stage A2. According to the adaptive law (10), E_{ref} is decreased in order to avoid skidding first (Stages B, C, and D), and then to optimize the energy (Stages D and E). Decreasing E_{ref} means lessening the movement intensity. From the figure, τ_{n-2}, η_2, and E_{T} fluctuate acutely after the change of E_{ref}, so the dwell time in each stage should be much longer than the transient time in order to eliminate the transient process. The on-line locomotion can not allow the robot to slowly test every possible E_{ref} in the finite time, so the adaptive step is tentative and the optimization is local.

The snake-like robot adapts to the unknown environment only based on the kinetic energy without the environment information ([6]) or dynamic model ([4]). The velocity of the control parameter change is much slower than the velocity of the transient process. Thus, the optimal adaptive law dose not influence the stability of the passive creeping. Finally, we have introduced the passive creeping with the environment adaptability completely as shown in Fig. 3.

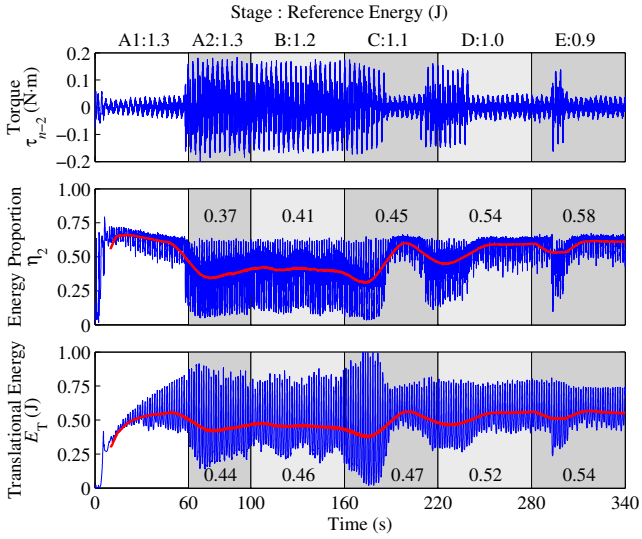

Fig. 11. An example about the adaptive process of the passive creeping. The initial stage A1 is in the startup with the reference energy E_{ref} being 1.3. In stage A2, the reference energy E_{ref}, the average energy proportion $\bar{\eta}_2$, and the average translational kinetic energy $\bar{E}_{\text{T}}$ are 1.3, 0.37, and 0.44, respectively. The rest can be read in the same manner. The environment parameters μ_{c}^n and μ_{c}^t, which are unknown to the snake-like robot, are 0.30 and 0.012 respectively. (See the attached video for more details.)

V. CONCLUSION

We have recalled the concept of the passive creeping, including the dissipation, transformation, and assignment of the energy in the serpentine locomotion. The control law of the passive creeping which integrates the energy process with the basic gait (i.e., dynamic shift) through the energy-based feedback has been introduced. The snake-like robot can implement the stable serpentine locomotion under the method. The local orbital stability has been explained by using the maximal Lyapunov exponent and the recurrence plot. Moveover, the adaptability to the environment has been analyzed, and the optimal adaptive control based on the kinetic energy is used to perfect the passive creeping. The particular advantage of the method is that the snake-like robot can adapt to the environments with different friction coefficients according to the energy state itself, so the environment information and the dynamic model are not needed to the adaptive process. In addition, each control parameter in the method has the explicit meaning and function. Finally, the measure of the kinetic energy is a difficulty, and we use an Optotrak Certus® motion capture system to obtain the kinetic energy in the experiment which is ongoing.

REFERENCES

[1] S. Hirose, *Biologically Inspired Robots (Snake-like Locomotor and Manipulator)*. Oxford: Oxford University Press, 1993.

[2] A. Crespi and A. Ijspeert, "Online optimization of swimming and crawling in an amphibious snake robot," *IEEE Trans. Robot.*, vol. 24, no. 1, pp. 75–87, 2008.

[3] R. L. Hatton and H. Choset, "Generating gaits for snake robots by annealed chain fitting and keyframe wave extraction," in *Proc. IEEE/RSJ Int. Conf. Intel. Rob. Sys.*, St. Louis, 2009, pp. 840–845.

[4] K. Watanabe, M. Iwase, S. Hatakeyama, and T. Maruyama, "Control strategy for a snake-like robot based on constraint force and verification by experiment," *Adv. Robot.*, vol. 23, pp. 907–937, 2009.

[5] H. Date and Y. Takita, "Adaptive locomotion of a snake like robot based on curvature derivatives," in *Proc. IEEE/RSJ Int. Conf. Intel. Rob. Sys.*, San Diego, 2007, pp. 3554–3559.

[6] K. Inoue, T. Sumi, and S. Ma, "CPG-based control of a simulated snake-like robot adaptable to changing ground friction," in *Proc. IEEE/RSJ Int. Conf. Intel. Rob. Sys.*, San Diego, 2007, pp. 1957–1962.

[7] S. Hasanzadeh and A. A. Tootoonchi, "Adaptive optimal locomotion of snake robot based on CPG-network using fuzzy logic tuner," in *Proc. IEEE Conf. Robot. Autom. Mechatron.*, Chengdu, 2008, pp. 187–192.

[8] Z. Wang, S. Ma, B. Li, and Y. Wang, "Passive creeping of a snake-like robot," in *Proc. IEEE Int. Conf. Robot. and Biomim.*, Guilin, 2009, pp. 57–62.

[9] ——, "Dynamic modeling for locomotion-manipulation of a snake-like robot by using geometric methods," in *Proc. IEEE/RSJ Int. Conf. Intel. Rob. Sys.*, St. Louis, 2009, pp. 3631–3636.

[10] H. Kantz and T. Schreiber, *Nonlinear Time Series Analysis*. Cambridge: Cambridge University Press, 2004.

[11] N. Marwan, M. C. Romano, M. Thiel, and J. Kurths, "Recurrence plots for the analysis of complex systems," *Physics Reports*, vol. 438, no. 5-6, pp. 237–329, 2007.